metals

MDPI

Article

Characterisation of Calcium- and Phosphorus-Enriched Porous Coatings on CP Titanium Grade 2 Fabricated by Plasma Electrolytic Oxidation

Krzysztof Rokosz [1], Tadeusz Hryniewicz [1,*], Sofia Gaiaschi [2], Patrick Chapon [2], Steinar Raaen [3], Kornel Pietrzak [1] and Winfried Malorny [4]

1 Division of BioEngineering and Surface Electrochemistry, Department of Engineering and Informatics Systems, Faculty of Mechanical Engineering, Koszalin University of Technology, Racławicka 15-17, PL 75-620 Koszalin, Poland; rokosz@tu.koszalin.pl (K.R.); kornel.pietrzak@s.tu.koszalin.pl (K.P.)

2 HORIBA France SAS, Avenue de la Vauve-Passage Jobin Yvon CS 45002, 91120 Palaiseau, France; sofia.gaiaschi@horiba.com (S.G.); patrick.chapon@horiba.com (P.C.)

3 Department of Physics, Norwegian University of Science and Technology (NTNU), Realfagbygget E3-124 Høgskoleringen 5, NO 7491 Trondheim, Norway; steinar.raaen@ntnu.no

4 Hochschule Wismar-University of Applied Sciences Technology, Business and Design, Faculty of Engineering, DE 23966 Wismar, Germany; winfried.malorny@hs-wismar.de

* Correspondence: Tadeusz.Hryniewicz@tu.koszalin.pl; Tel.: +48-94-347-8244

Received: 1 August 2017; Accepted: 1 September 2017; Published: 8 September 2017

Abstract: In the paper, Scanning Electron Microscopy (SEM), Energy-dispersive X-ray Spectroscopy (EDS), X-ray Photoelectron Spectroscopy (XPS), and Glow Discharge Optical Emission Spectroscopy (GDOES) analyses of calcium- and phosphorus-enriched coatings obtained on commercial purity (CP) Titanium Grade 2 by plasma electrolytic oxidation (PEO), known also as micro arc oxidation (MAO), in electrolytes based on concentrated phosphoric acid with calcium nitrate tetrahydrate, are presented. The preliminary studies were performed in electrolytes containing 10, 300, and 600 g/L of calcium nitrate tetrahydrate, whereas for the main research the solution contained 500 g/L of the same hydrated salt. It was found that non-porous coatings, with very small amounts of calcium and phosphorus in them, were formed in the solution with 10 g/L $Ca(NO_3)_2 \cdot 4H_2O$, whereas the other coatings, fabricated in the consecutive electrolytes containing from 300 up to 650 g/L $Ca(NO_3)_2 \cdot 4H_2O$, were porous. Based on the GDOES data, it was also found that the obtained porous PEO coating may be divided into three sub-layers: the first, top, porous layer was the thinnest; the second, semi-porous layer was about 12 times thicker than the first; and the third, transition sub-layer was about 10 times thicker than the first. Based on the recorded XPS spectra, it was possible to state that the top 10-nm layer of porous PEO coatings included chemical compounds containing titanium (Ti^{4+}), calcium (Ca^{2+}), as well as phosphorus and oxygen (PO_4^{3-} and/or HPO_4^{2-} and/or $H_2PO_4^{-}$, and/or $P_2O_7^{4-}$).

Keywords: CP Titanium Grade 2; plasma electrolytic oxidation (PEO); micro arc oxidation (MAO); calcium nitrate tetrahydrate; SEM; EDS; XPS; GDOES

1. Introduction

Nowadays, light metals such as titanium [1–4], niobium [5–9], tantalum [10–15], and their alloys [16–22], after electrochemical treatment (electropolishing and/or plasma electrolytic oxidation), may be used as biomaterials (implant materials) because of their mechanical properties [23–27], good corrosion resistance [28–31] in body fluids, and osteointegration [32–34]. The electropolishing

processes, such as standard electropolishing (EP) [35–39], magnetoelectropolishing (MEP) [40–43], high-current density electropolishing (HDEP) [44–46], and high-voltage electropolishing (HVEP) [47], allow for the formation of nano-layers on a metal surface, which may consist of metal phosphates/sulfates with additives originating from solution [39] studied for chemical composition [48–52] and surface hydration [53,54], as well as for mechanical properties [24]. To obtain porous micro-layers as coatings on light metals and alloys, plasma electrolytic oxidation (PEO), known also in the literature as micro arc oxidation (MAO) [1–4,7–22], should be used.

The main advantage of the PEO process is the formation of porous coatings which are enriched in ions originating from the electrolyte used [55]. This is a very important characteristic, because the biomaterials' top layers (in this case the PEO coating) act as transition layers between bone structure and metal, and they should mimic the bone tissue. Therefore, the coatings' bone-like structure should be non-stoichiometric and enriched mainly in calcium (Ca^{2+}) and phosphorus ($H_2PO_4^-$, HPO_4^{2-}, PO_4^{3-}). It should be noted that in biological apatites, the Ca^{2+} ions may be substituted by other ions, e.g., Mg^{2+}, Sr^{2+}, Na^+, K^+, Si^{4+}, whereas PO_4^{3-} groups may be substituted by CO_3^{2-} [56,57]. It is also possible to find in the literature a chemical formula of bone, i.e., $Ca_{8.3}(PO_4)_{4.3}(CO_3)_x(HPO_4)_y(OH)_3$, where $x + y \approx 1.7$, knowing that x increases and y decreases with age [56]. Additionally, it may be stated that other chemical elements may be used in substitution of the calcium Ca^{2+} ions. These ions, among others, may be bactericidal copper (Cu^{2+}, Cu^+) [22,58–62] or silver (Ag^+) [63–66]. In addition, it was determined that the roughness parameters [67,68] may be used to describe the porosity of the top surface of porous coatings, i.e., the higher the voltage used in the PEO process, the higher the roughness will be [19,61], which may be explained by the fact that for large pores, a high surface roughness is recorded.

In the present paper, new porous coatings enriched in calcium and phosphorus and obtained in an electrolyte based on concentrated phosphoric 85% H_3PO_4 acid and calcium nitrate tetrahydrate $Ca(NO_3)_2{\cdot}4H_2O$ under DC voltage conditions, with and without pulsation, is presented. Analysis of the available literature shows that most commonly used electrolytes containing calcium ions, which may be used in PEO treatments of titanium and its alloys, contain in themselves inter alia calcium dihydrohypophosphite [34], calcium acetate hydrate [69], disodium hydrogen phosphate [70], Ca-β-glycerophosphate [71], calcium acetate [72], and tricalcium phosphate [73].

2. Method

The plasma electrolytic oxidation (micro arc oxidation) process was used for the treatment of samples of commercial purity (CP) Titanium Grade 2 with dimensions of 10 mm × 10 mm × 2 mm. The plasma electrolytic oxidation (PEO) during the preliminary studies was performed with an average voltage of 450 ± 46 V, and pulsation at a frequency of 300 Hz during 3 min of treatment by using a three-phase transformer with six diodes of Greatz Bridge in electrolytes containing 10, 300, and 600 g/L of calcium nitrate tetrahydrate dissolved in 1000 mL concentrated 85% analytically pure H_3PO_4 (98 g/mole). The main studies were performed at 500 $V_{DC,}$ 575 V_{DC}, 650 V_{DC} voltages without any pulsation by using a commercial DC power supply PWR 1600 H, Multi Range DC Power Supply 1600 W, 0–650 V/0–8 A. The electrolyte, used in the main studies, consisted of a concentrated 85% analytically pure H_3PO_4 (98 g/mole) acid, 1000 mL, with 500 g of calcium nitrate $Ca(NO_3)_2{\cdot}4H_2O$ dissolved in it.

A scanning electron microscope Quanta 250 FEI (Field Electron and Iron Company, Hillsboro, OR, USA) with Low Vacuum and ESEM mode and a field emission cathode, as well as an Energy-dispercive X-ray Spectroscopy (EDS, Silicon Drift Detectors: Keith Thompson, Thermo Fisher Scientific, Madison, WI, USA), system in a Noran System Six with nitrogen-free silicon drift detector, were used.

The Glow Discharge Optical Emission Spectroscopy (GDOES) measurements on PEO-oxidized titanium samples were performed on a Horiba Scientific GD Profiler 2 instrument (HORIBA Scientific, Palaiseau, France) using radio frequency (RF) asynchronous pulse generator under the plasma conditions (pressure: 700 Pa, power: 40 W, frequency: 3000 Hz, duty cycle: 0.25, anode diameter:

4 mm). The GDOES signals of calcium (423 nm), phosphorus (178 nm), oxygen (130 nm), nitrogen (149 nm), hydrogen (122 nm), and titanium (365 nm) were measured [74–76].

The X-ray Photoelectron Spectroscopy (XPS) measurements on studied samples' surfaces were performed by means of a SCIENCE SES 2002 instrument (SCIENTA AB, ScientaOmicron, Uppsala, Sweden) using a monochromatic (Gammadata-Scienta) Al Kα (hν = 1486.6 eV) X-ray source (18.7 mA, 13.02 kV). Scan analyses were carried out with an analysis area of 1 × 3 mm and a pass energy of 500 eV with the energy step 0.2 eV and step time 200 ms. The binding energy of the spectrometer was calibrated by the position of the Fermi level on a clean metallic sample. The power supplies were stable and of high accuracy. The experiments were carried out in an ultra-high vacuum system with a base pressure of about 6×10^{-8} Pa. The XPS spectra were recorded in normal emission. For the XPS analyses, CasaXPS 2.3.14 software (Shirley background type) [77], with the help of XPS tables [78], was used. All the binding energy values presented in this paper were charge corrected to C 1s at 284.8 eV.

3. Results

In Figure 1, the SEM images with 500× (a), 1000× (b), 5000× (c), and 10,000× (d) magnifications as well as the EDS spectrum (e) of the porous coating formed on CP Titanium Grade 2 after PEO treatment at a voltage of 450 V with a pulsation of 300 Hz after 3 min in an electrolyte containing 10 g of calcium nitrate tetrahydrate $Ca(NO_3)_2 \cdot 4H_2O$ in 1000 mL of concentrated 85% phosphoric acid H_3PO_4, are presented. The obtained surface is not porous with small islands within a dozen of micrometers, which contain phosphorus (ca. 0.5 at %) and calcium (ca. 0.1 at %) compounds, resulting in a calcium-to-phosphorus Ca/P ratio equal to ca. 0.2. However, the EDS analysis shows that the amount of calcium in most places, besides the mentioned islands, is null.

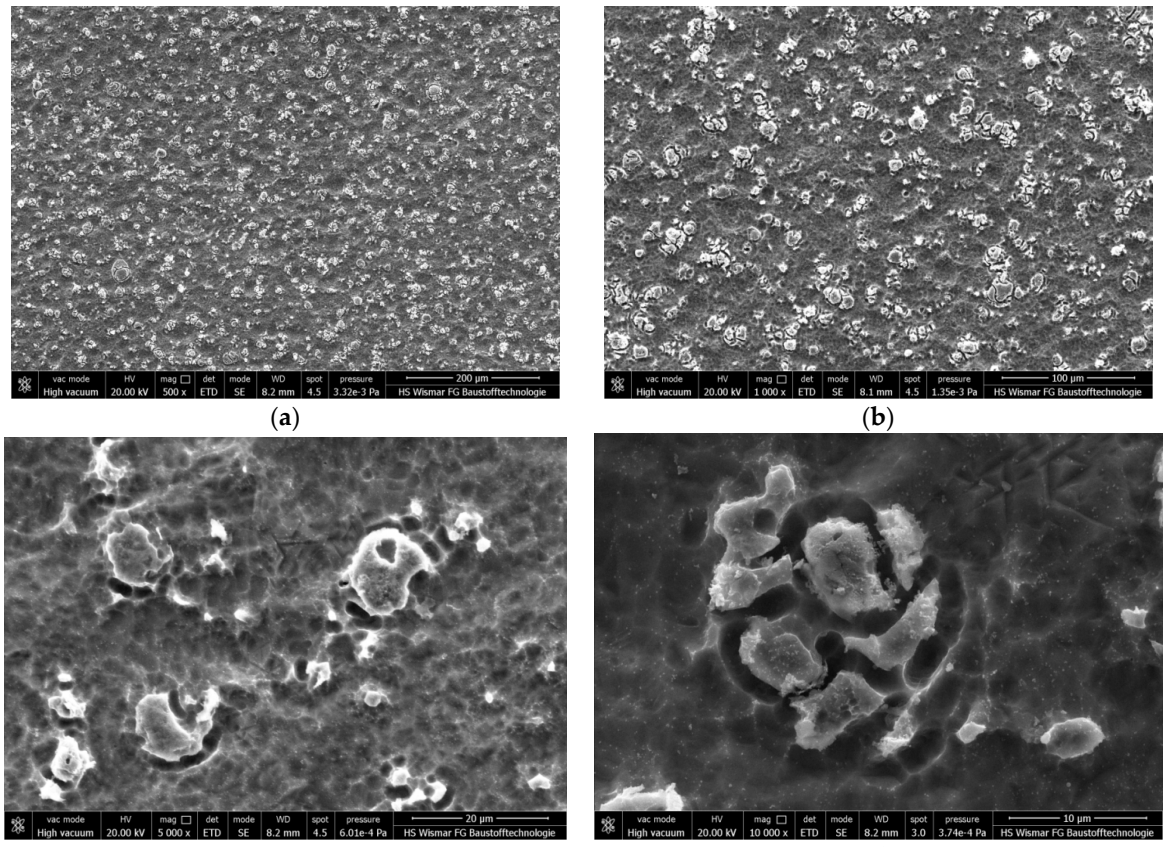

Figure 1. *Cont.*

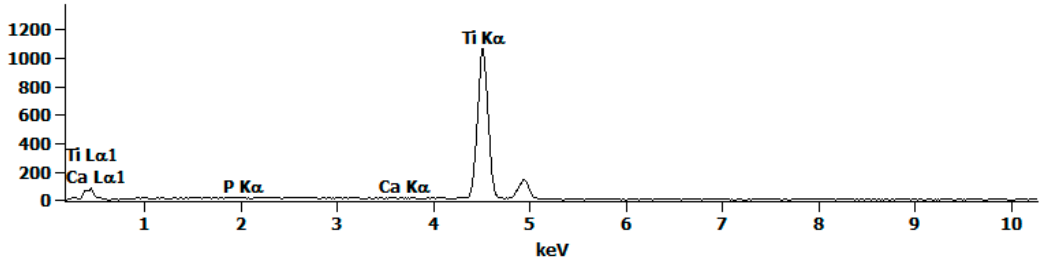

(**e**)

Figure 1. Scanning Electron Microscopy (SEM) pictures (**a**–**d**) and Energy-dispersive X-ray Spectroscopy (EDS) spectrum (**e**) of the porous coating formed on commercial purity (CP) Titanium Grade 2 after Plasma Electrolytic Oxidation (PEO) treatment at a voltage of 450 V in 10 g $Ca(NO_3)_2 \cdot 4H_2O$ in 1000 mL H_3PO_4 electrolyte. Magnifications: (**a**) 500×, (**b**) 1000×, (**c**) 5000×, (**d**) 10,000×.

In Figure 2, the SEM images with 500× (a), 1000× (b), 5000× (c), and 10,000× (d) magnifications as well as the EDS spectrum (e) of the porous coating formed on CP Titanium Grade 2 after PEO treatment at a voltage of 450 V with a pulsation of 300 Hz after 3 min in an electrolyte containing 300 g of calcium nitrate tetrahydrate $Ca(NO_3)_2 \cdot 4H_2O$ in 1000 mL of concentrated phosphoric acid H_3PO_4, are presented. The obtained coatings are porous and contain calcium (3.7 ± 0.6 at %; median: 3.8 at %, range: 1.9 at %), phosphorus (45 ± 0.9 at %; median: 45.1 at %, range: 2.7 at %), and titanium (51.2 ± 1.3 at %; median: 51.1 at %, range: 3.8 at %), which may have originated both from coatings as well as from the matrix. Based on the EDS data, calcium-to-phosphorus Ca/P ratios equal to 0.08 ± 0.01 (median: 0.09, range: 0.04) were found.

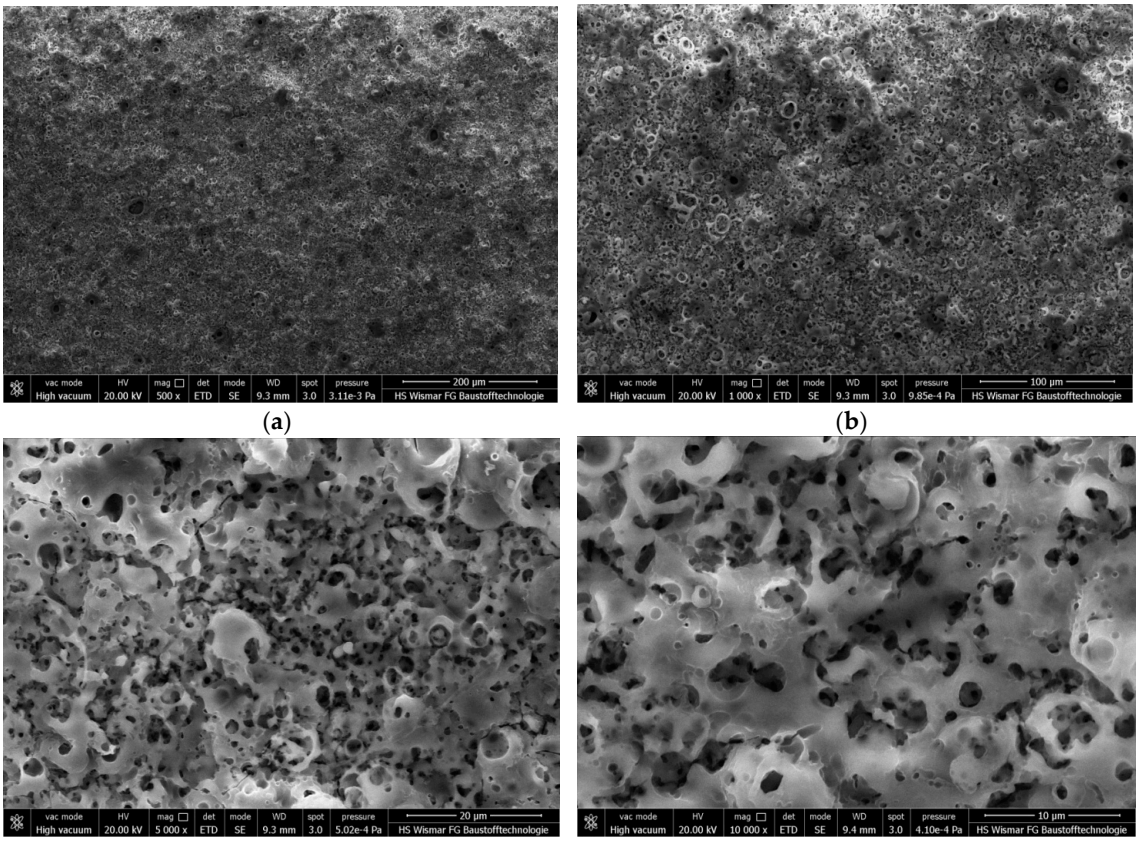

(**a**) (**b**)

(**c**) (**d**)

Figure 2. *Cont.*

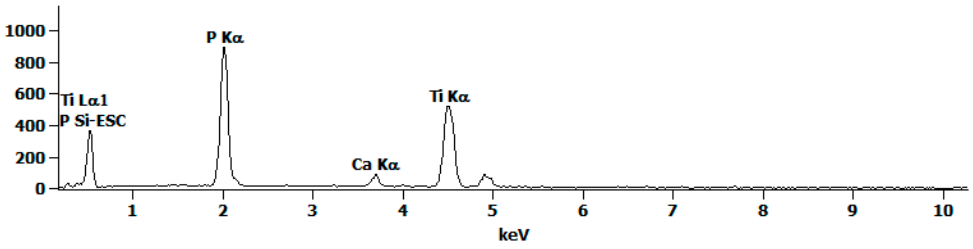

(**e**)

Figure 2. SEM pictures (**a**–**d**) and EDS spectrum (**e**) of the porous coating formed on CP Titanium Grade 2 after PEO treatment at voltage of 450 V in 300 g $Ca(NO_3)_2 \cdot 4H_2O$ in 1000 mL H_3PO_4 electrolyte. Magnifications: (**a**) 500×, (**b**) 1000×, (**c**) 5000×, (**d**) 10,000×.

In Figure 3, the SEM images with 500× (a), 1000× (b), 5000× (c), and 10,000× (d) magnifications as well as the EDS spectrum (e) of the porous coating formed on CP Titanium Grade 2 after PEO treatment at a voltage of 450 V with a pulsation of 300 Hz after 3 min in an electrolyte containing 600 g of calcium nitrate tetrahydrate $Ca(NO_3)_2 \cdot 4H_2O$ in 1000 mL of concentrated phosphoric acid H_3PO_4, are presented. The obtained coatings are porous and contain calcium (7.4 ± 0.6 at %; median: 7.6 at %, range: 1.7 at %), phosphorus (51.8 ± 1.5 at %; median: 51.9 at %, range: 3.3 at %), and titanium (40.7 ± 2.0 at %; median: 40.1 at %, range: 4.6 at %), which may have originated both from the coatings as well as from the matrix. Based on the EDS data, calcium-to-phosphorus Ca/P ratios equal to 0.15 ± 0.01 (median: 0.15, range: 0.03) were found. The decreasing amount of titanium from the EDS analysis indicates that with increasing amount of calcium nitrate tetrahydrate from 10 g/L up to 600 g/L in the electrolyte, an increase in the coating thickness is observed. In addition, it was found that the ratio Ca/P can be expressed as $Ca/P = 2.4 \times 10^{-4} \times x$, where x (g/L) is the amount of calcium nitrate tetrahydrate in the electrolyte.

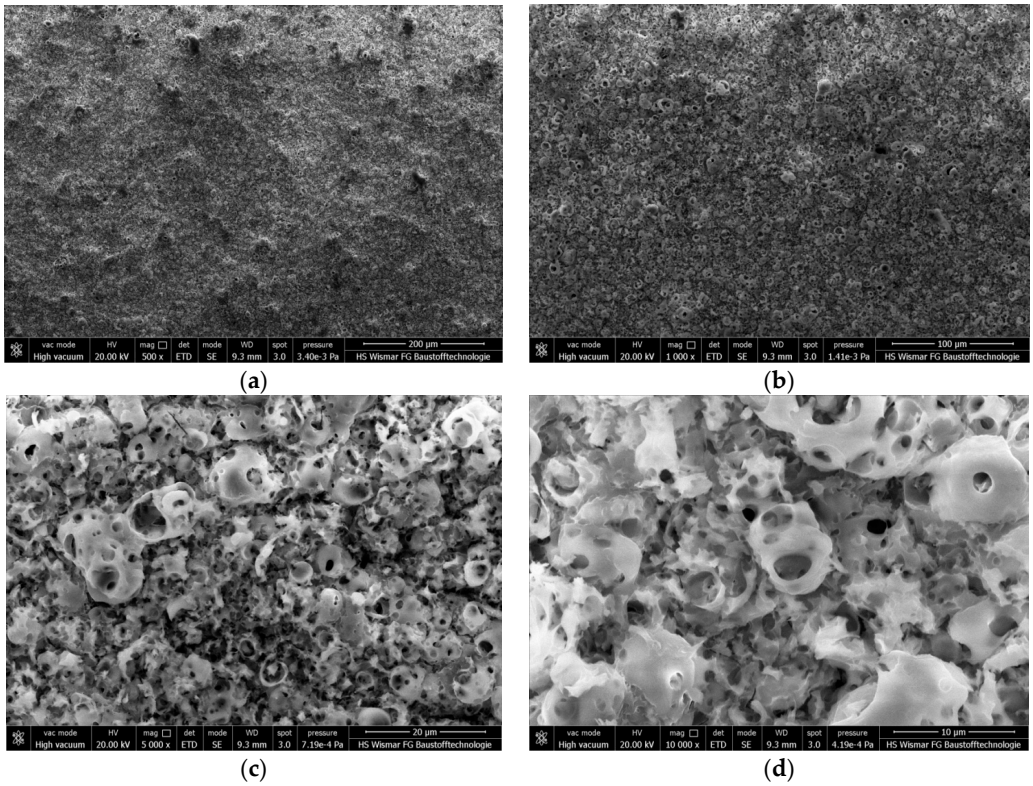

(**a**) (**b**)

(**c**) (**d**)

Figure 3. *Cont.*

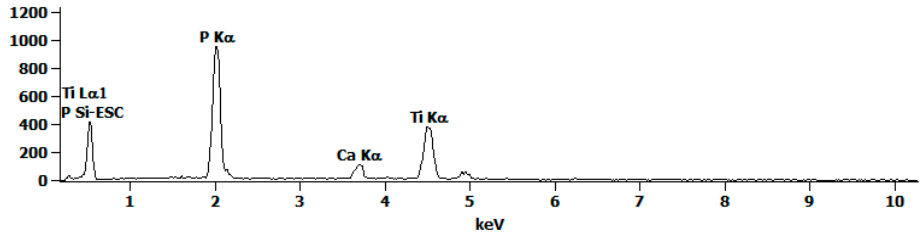

(**e**)

Figure 3. SEM pictures (**a**–**d**) and EDS spectrum (**e**) of the porous coating formed on CP Titanium Grade 2 after PEO treatment at a voltage of 450 V in 600 g $Ca(NO_3)_2{\cdot}4H_2O$ in 1000 mL H_3PO_4 electrolyte. Magnifications: (**a**) 500×, (**b**) 1000×, (**c**) 5000×, (**d**) 10,000×.

In Figure 4, the GDOES signals with their derivates of calcium (a), phosphorus (b), oxygen (c), hydrogen (d), carbon (e), nitrogen (f), and titanium (g) of the porous coating formed on CP Titanium Grade 2 after PEO treatment at a voltage of 450 V in 10 g, 300 g, and 600 g $Ca(NO_3)_2{\cdot}4H_2O$ in 1000 mL H_3PO_4 electrolytes, are presented. At first glance, it can be observed that the thickest porous coating enriched with calcium, phosphorus, and oxygen was obtained with the PEO treatment in an electrolyte containing 600 g/L of calcium nitrate tetrahydrate. As it was presented in the EDS results (Figure 1) with the coating/layer obtained from the solution with 10 g/L $Ca(NO_3)_2{\cdot}4H_2O$, the GDOES signals of oxygen, carbon, and nitrogen may suggest that the formed surface layer consists of organic contaminations with very small amounts of calcium-phosphate-titanium compounds. It is worth noting [19,22] that the obtained coatings may be divided into three sub-layers, i.e., the first one with open and organically contaminated pores; the second semi-porous one, which has a different thickness dependent on calcium nitrate tetrahydrate amount in the electrolyte used; and the third transition sub-layer. The thicknesses of the first sub-layer for all obtained layers/coatings are about the same and correspond to 40 s of GDOES sputtering time. For the sample treated in the electrolyte with 10 g/L $Ca(NO_3)_2{\cdot}4H_2O$, only the two sub-layers (the first and third) were found, while for the next two treatments, i.e., with 300 g/L and 600 g/L of $Ca(NO_3)_2{\cdot}4H_2O$, all three sub-layers were recorded. It has to be noted that the second sub-layer has a different thickness, and depends on the electrolyte used. The higher the amount of calcium nitrate tetrahydrate in the solution, the thicker the second/third sub-layer will be, i.e., corresponding with 360 s/350 s and 510 s/400 s of sputtering time for 300 and 600 g/L of $Ca(NO_3)_2{\cdot}4H_2O$, respectively. Based on carbon and hydrogen GDOES signals and their derivates, it is possible to determine the point at which the porosity decreases down to null. They are observed as the local maxima in carbon and hydrogen signals, what may be explained as organic contaminations from air. Thus, it has to be inferred that all pores are connected together and the end of porosity is located inside the third-transitional layer of PEO coating. That place/dimple may be used e.g., for drug delivery. All of the sub-layers are enriched in calcium, phosphorus, oxygen, and small amounts of nitrogen and titanium. Taking into account the fact that calcium nitrate tetrahydrate $Ca(NO_3)_2{\cdot}4H_2O$ and phosphoric acid H_3PO_4 were used for the PEO treatment of the electrolyte, it should be noted that the coatings are built of titanium (Ti^{4+}), calcium (Ca^{2+}), and phosphate ($PO_4{}^{3-}$) and/or hydrogen phosphate ($HPO_4{}^{2-}$) and/or dihydrogen phosphate ($H_2PO_4{}^{-}$) and/or pyrophosphates ($P_2O_7{}^{4-}$).

In Figure 5, the SEM images with 500× (a), 1000× (b), 5000× (c), and 10,000× (d) magnifications as well as the EDS spectrum (e) of the porous coating formed on CP Titanium Grade 2 after PEO treatment at a voltage of 450 V_{DC} without any pulsation after 3 min in an electrolyte containing 500 g of calcium nitrate tetrahydrate $Ca(NO_3)_2{\cdot}4H_2O$ in 1000 mL of concentrated phosphoric acid H_3PO_4, are presented. The obtained coatings are porous with "volcano pores", which contain calcium (8.8 ± 0.3 at %; median: 8.8 at %, range: 1.5 at %), phosphorus (49.9 ± 0.9 at %; median: 50.6 at %, range: 4.1 at %), and titanium (40.5 ± 1.2 at %; median: 40.7 at %, range: 5.2 at %), and may have originated both from the coatings as well as from the matrix. Based on the EDS data, a calcium-to-phosphorus Ca/P ratio

equal to 0.18 ± 0.01 (median: 0.18, range: 0.01) was found. Therefore, it follows that with using DC voltage (450 V_{DC}) without any pulsation and an electrolyte with a smaller amount (500 g/L) of calcium nitrate tetrahydrate, it is possible to obtain more calcium in coatings than it was using the three-phase transformer with six diodes of Greatz Bridge and the solution with 600 g/L of $Ca(NO_3)_2 \cdot 4H_2O$.

In Figure 6, the SEM images with 500× (a), 1000× (b), 5000× (c), and 10,000× (d) magnifications as well as the EDS spectrum (e) of the porous coating formed on CP Titanium Grade 2 after PEO treatment at a voltage of 500 V_{DC} without any pulsation after 3 min in an electrolyte containing 500 g of calcium nitrate tetrahydrate $Ca(NO_3)_2 \cdot 4H_2O$ in 1000 mL of concentrated phosphoric acid H_3PO_4, are presented. The obtained coatings are porous, and more "volcano pores" with bigger diameters were found on them than on the coatings treated at 450 V_{DC}. Based on the EDS results, it is possible to state that the porous coatings contain calcium (11 ± 1.5 at %; median: 11 at %, range: 5.8 at %), phosphorus (50.5 ± 1.0 at %; median: 50.4 at %, range: 3.4 at %), and titanium (38.5 ± 1.1 at %; median: 38.7 at %, range: 4.3 at %). Calcium-to-phosphorus Ca/P ratios equal to 0.22 ± 0.03 (median: 0.22, range: 0.12) were obtained. From the results, it seems that the PEO treatment at 500 V_{DC} allows the formation of coatings with higher amount of calcium compared to those described before. Therefore, the other two higher potentials, i.e., 550 V_{DC} and 650 V_{DC}, were used in order to find even higher Ca/P ratios.

In Figure 7, the SEM images with 500× (a), 1000× (b), 5000× (c), and 10,000× (d) magnifications as well as the EDS spectrum (e) of the porous coating formed on Titanium Grade 2 after PEO treatment at a voltage of 550 V_{DC} without any pulsation after 3 min in an electrolyte containing 500 g of calcium nitrate tetrahydrate $Ca(NO_3)_2 \cdot 4H_2O$ in 1000 mL of concentrated phosphoric acid H_3PO_4, are presented. The obtained coatings are porous and look similar to those obtained after PEO treatment at 500 V_{DC}. The porous coatings formed at 550 V_{DC} contain calcium (10 ± 0.7 at %; median: 10 at %, range: 2.4 at %), phosphorus (53.6 ± 1.8 at %; median: 53.1 at %, range: 6.2 at %), and titanium (36.4 ± 1.8 at %; median: 36.6 at %, range: 5.6 at %). The calcium-to-phosphorus Ca/P ratios were found to be 0.9 ± 0.02 (median: 0.19, range: 0.05). From this, it follows that further increasing the voltage leads to a decrease of the amount of calcium in the PEO coating.

In Figure 8, the SEM images with 500× (a), 1000× (b), 5000× (c), and 10,000× (d) magnifications as well as the EDS spectrum (e) of the porous coating formed on CP Titanium Grade 2 after PEO treatment at a voltage of 650 V_{DC} without any pulsation after 3 min in an electrolyte containing 500 g of calcium nitrate tetrahydrate $Ca(NO_3)_2 \cdot 4H_2O$ in 1000 mL of concentrated phosphoric acid H_3PO_4, are presented. The obtained coatings are porous but it should be noted that they exhibit the most developed area among all of those surveyed, and look similar to those obtained after PEO treatment at 500 V_{DC}. The chemical composition of the formed PEO coating was as follows: calcium (9.8 ± 0.3 at %; median: 9.8 at %, range: 1.3 at %), phosphorus (50.1 ± 0.7 at %; median: 50.4 at %, range: 2.6 at %), and titanium (40.1 ± 0.9 at %; median: 39.8 at %, range: 3.0 at %). The calcium-to-phosphorus Ca/P ratios were found to be equal to 0.19 ± 0.01 (median: 0.2, range: 0.02). This confirms that further increasing voltage up to 650 V_{DC} results in a decrease of the amount of calcium in the formed PEO coating.

In Figure 9, XPS spectra of coatings formed on CP Titanium Grade 2 after PEO treatment at voltages of 450 V_{DC}, 500 V_{DC}, and 650 V_{DC} after 3 min in 500 g/L of $Ca(NO_3)_2 \cdot 4H_2O$ in 1000 mL H_3PO_4 electrolyte, are presented. The obtained XPS results clearly show that in the top layer (10 nm) there is titanium (Ti^{4+}), calcium (Ca^{2+}), as well as phosphorus and oxygen with hydrogen, most likely as PO_4^{3-} and/or HPO_4^{2-} and/or $H_2PO_4^{-}$, and/or $P_2O_7^{4-}$ present, which is confirmed by the binding energies, i.e., Ti $2p_{3/2}$ (460–460.4 eV), Ca $2p_{3/2}$ (347.4–347.7 eV), P 2p (133.9–134.4 eV), and O 1s (531.5–531.6 eV). In addition, based on the peaks of oxygen O 1s and phosphorus P 2p, the oxygen-to-phosphorus O/P ratios, which are within the range of 1.4–1.7, for all three coatings were found. Taking into account the information from the EDS studies for DC voltages without pulsation, which indicated that Ca/P ratios for all coatings were equal to ca. 0.2, one may conclude that the obtained PEO coating compounds are not stoichiometric.

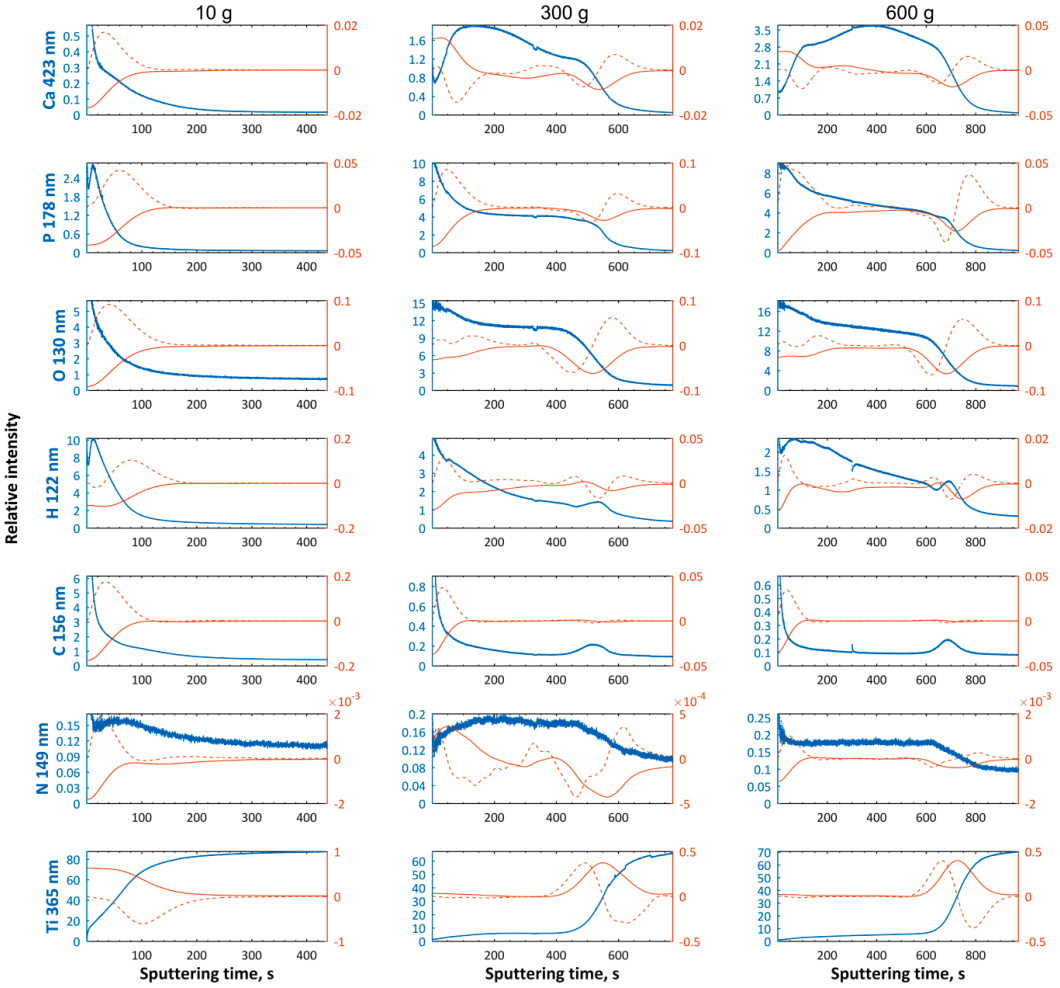

Figure 4. Glow Discharge Optical Emission Spectroscopy (GDOES) signals of calcium (Ca), phosphorus (P), oxygen (O), hydrogen (H), carbon (C), nitrogen (N), and titanium (Ti) of the porous coating formed on CP Titanium Grade 2 after PEO treatment at a voltage of 450 V in 10 g, 300 g, and 600 g $Ca(NO_3)_2 \cdot 4H_2O$ in 1000 mL H_3PO_4 electrolytes; blue continuous line—GDOES signal, red continuous line—first derivative, red dotted line—second derivative.

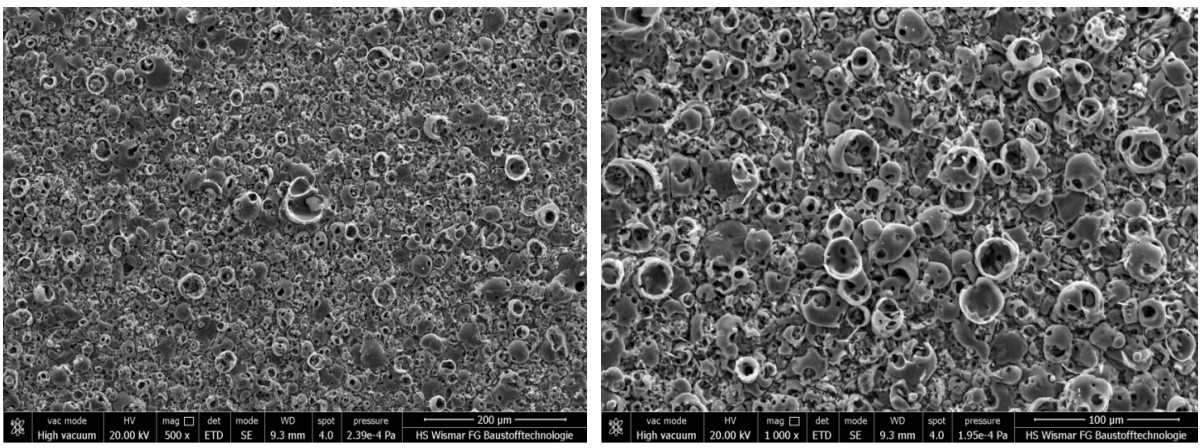

(**a**) (**b**)

Figure 5. *Cont.*

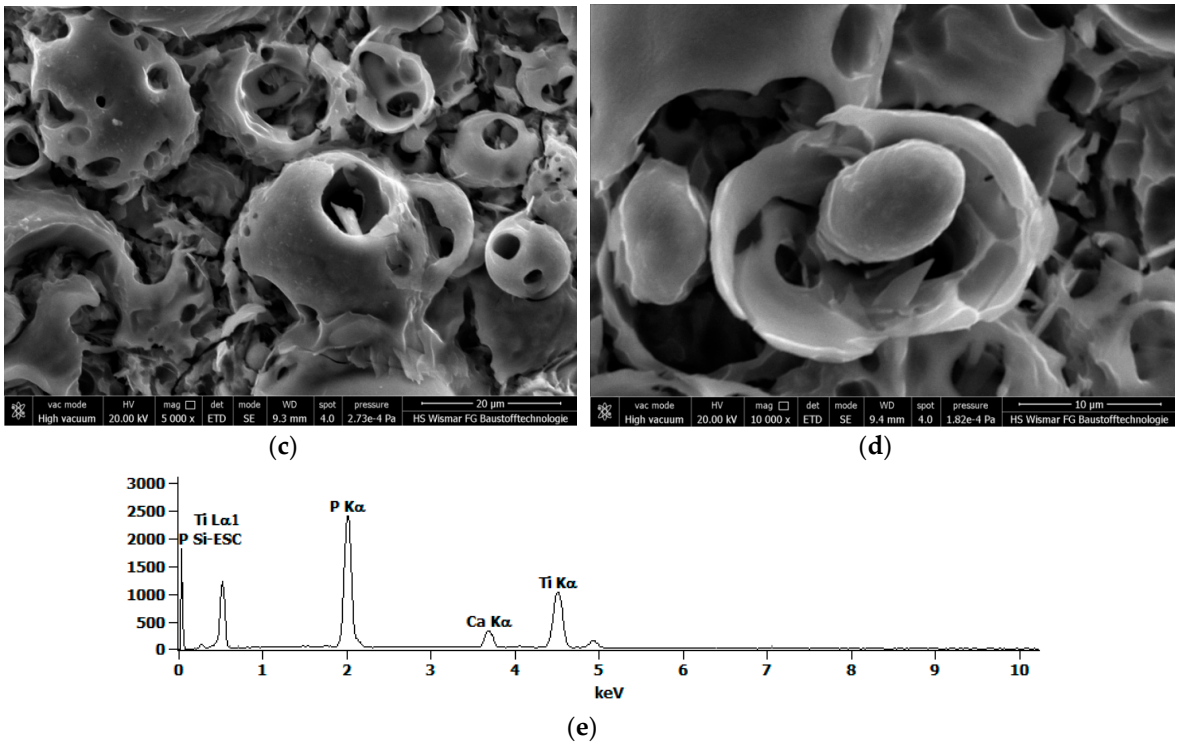

Figure 5. SEM pictures (**a**–**d**) and EDS spectrum (**e**) of the porous coating formed on CP Titanium Grade 2 after PEO treatment at a voltage of 450 V_{DC} in 500 g $Ca(NO_3)_2 \cdot 4H_2O$ in 1000 mL H_3PO_4 electrolyte. Magnifications: (**a**) 500×, (**b**) 1000×, (**c**) 5000×, (**d**) 10,000×.

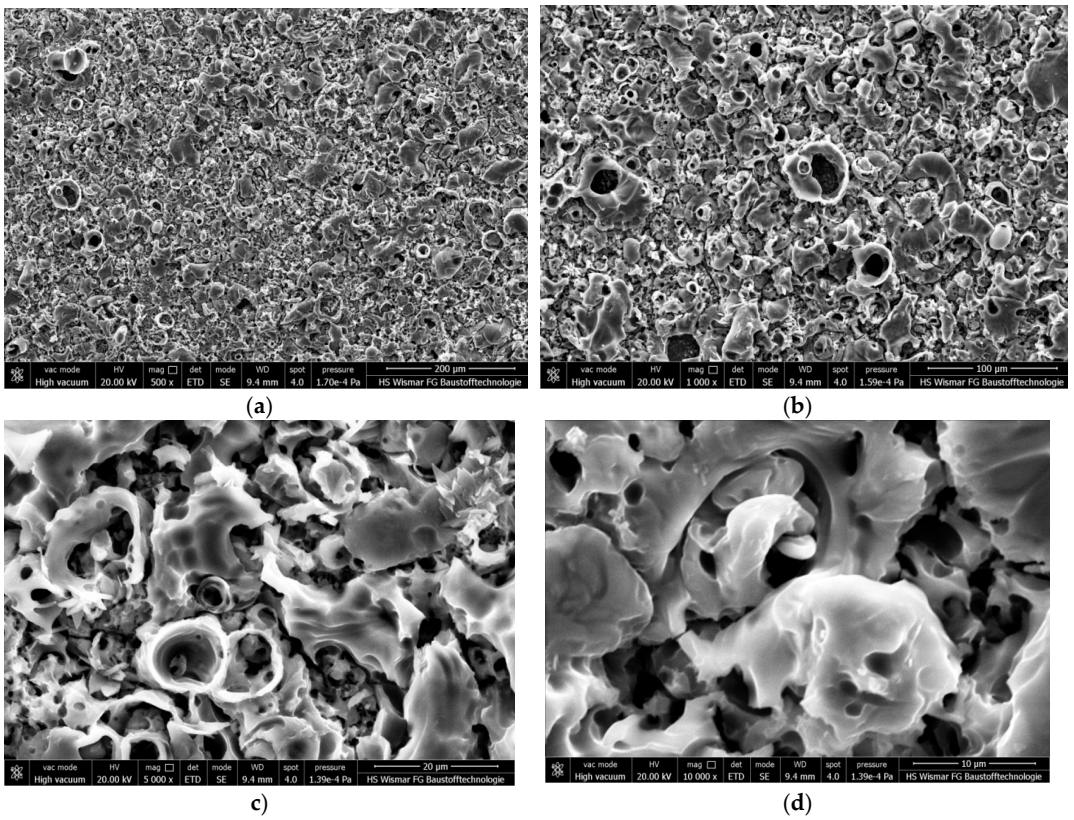

Figure 6. *Cont.*

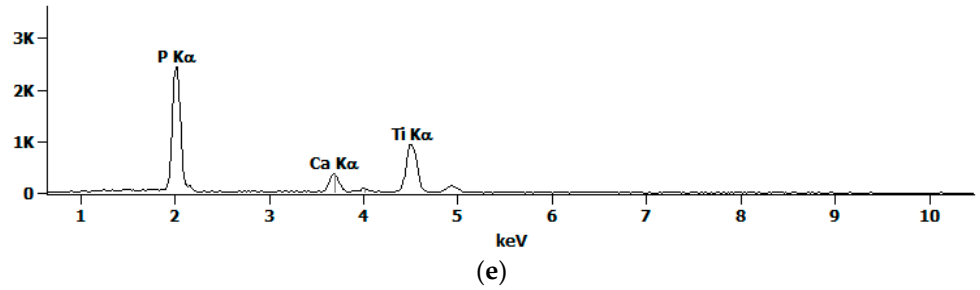

(**e**)

Figure 6. SEM pictures (**a**–**d**) and EDS spectrum (**e**) of the porous coating formed on CP Titanium Grade 2 after PEO treatment at a voltage of 500 V_{DC} in 500 g $Ca(NO_3)_2 \cdot 4H_2O$ in 1000 mL H_3PO_4 electrolyte. Magnifications: (**a**) 500×, (**b**) 1000×, (**c**) 5000×, (**d**) 10,000×.

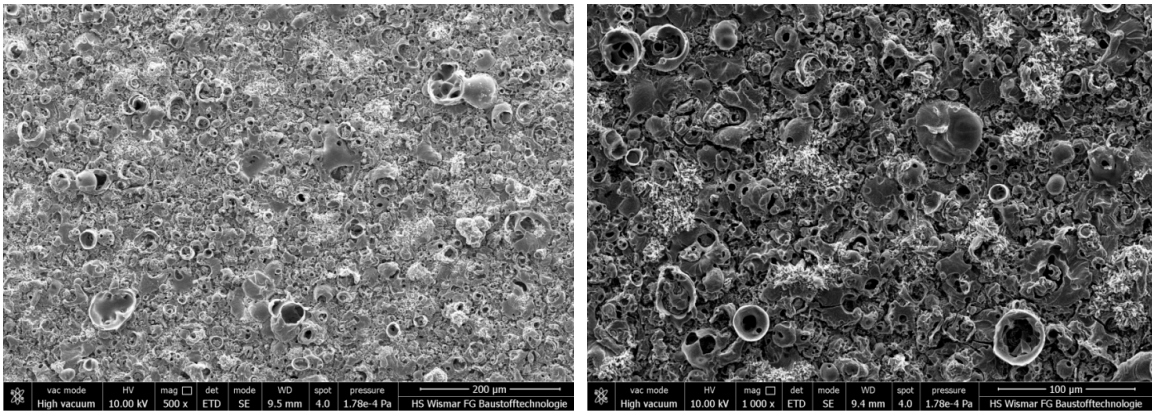

(**a**)

(**b**)

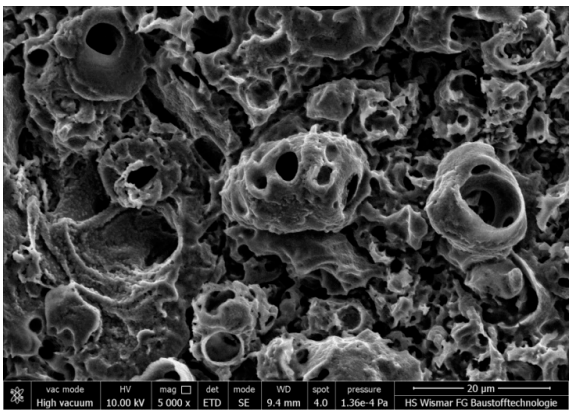

(**c**)

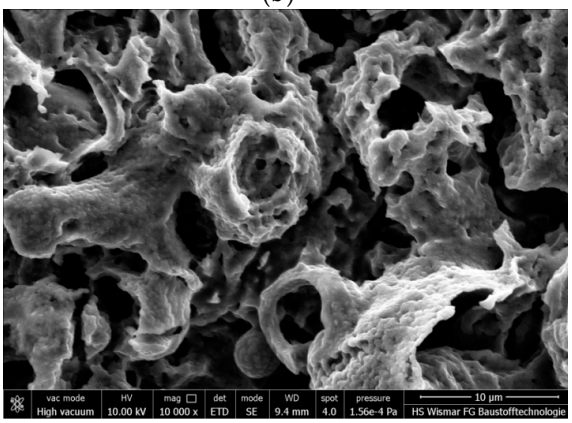

(**d**)

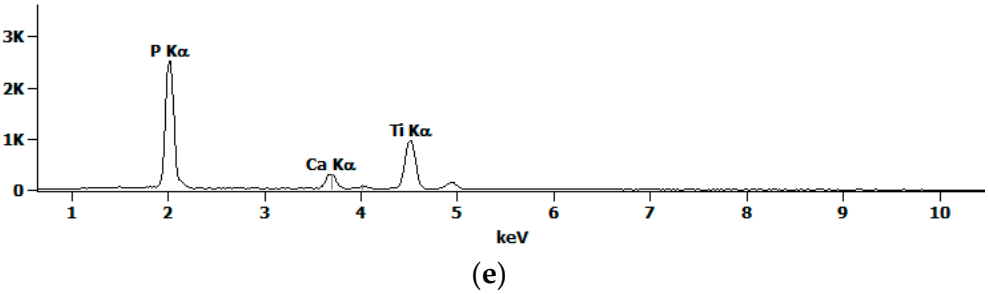

(**e**)

Figure 7. SEM pictures (**a**–**d**) and EDS spectrum (**e**) of the porous coating formed on CP Titanium Grade 2 after PEO treatment at a voltage of 550 V_{DC} in 500 g $Ca(NO_3)_2 \cdot 4H_2O$ in 1000 mL H_3PO_4 electrolyte. Magnifications: (**a**) 500×, (**b**) 1000×, (**c**) 5000×, (**d**) 10,000×.

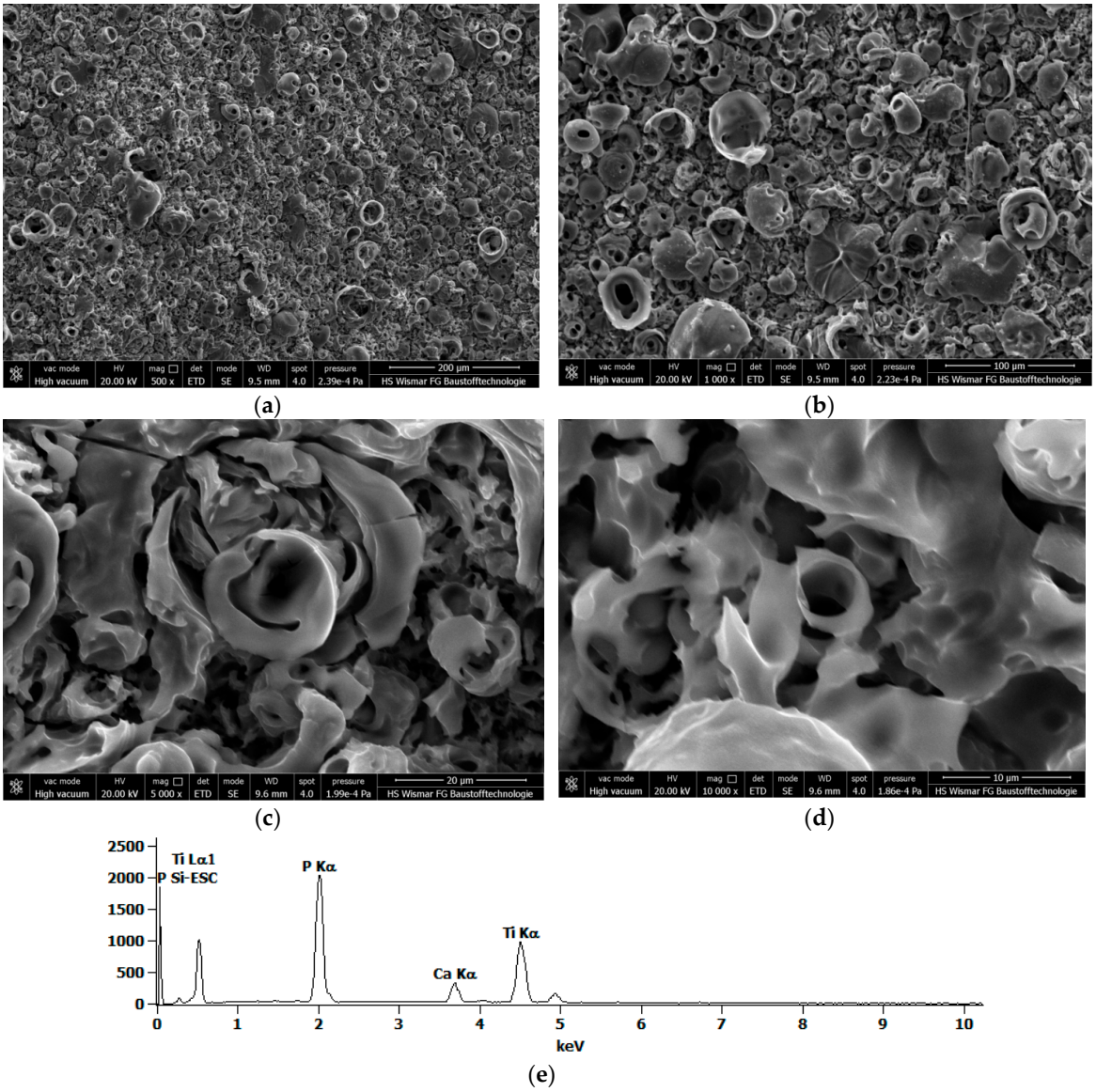

Figure 8. SEM pictures (**a**–**d**) and EDS spectrum (**e**) of the porous coating formed on CP Titanium Grade 2 after PEO treatment at a voltage of 650 V_{DC} in 500 g $Ca(NO_3)_2 \cdot 4H_2O$ in 1000 mL H_3PO_4 electrolyte. Magnifications: (**a**) 500×, (**b**) 1000×, (**c**) 5000×, (**d**) 10,000×.

Plasma electrolytic oxidation (micro arc oxidation) was developed on CP Titanium Grade 2 to obtain porous, calcium- and phosphorus-enriched, coatings to be used as biocompatible surfaces as well as for automotive and industrial catalysts. SEM, EDS, XPS, and GDOES techniques were used to study the PEO coatings. In the experiments, two types of DC voltages, i.e., with and without pulsation, were used to fabricate these PEO coatings. The preliminary studies were performed on samples, on which the porous coatings were formed in electrolytes containing 10, 300, and 600 g/L of calcium nitrate tetrahydrate with the use of a three-phase transformer with six diodes of Greatz Bridge. The obtained results clearly show that the coating formed in the solution with 10 g/L $Ca(NO_3)_2 \cdot 4H_2O$ is not porous and that there are islands on it containing mainly calcium, phosphorus, and oxygen, for which calcium-to-phosphate Ca/P ratio is equal to 0.2. The coatings obtained in electrolytes with 300 and 600 g/L calcium nitrate tetrahydrate are porous and their Ca/P ratios are equal to 0.08 and 0.15, respectively. Based on the analysis of the GDOES results, one may conclude that the obtained PEO coatings may be divided into sub-layers, i.e., the first layer with open sharp edges of pores (40 s of

sputtering time), the second, semi-porous layer, enriched in calcium with thicknesses corresponding to sputtering time from 360 s to 510 s, and the third transition layer (350–400 s). It was also found that the higher the amount of calcium nitrate tetrahydrate in the solution, the thicker the second and third sub-layers become. Based on the preliminary results, a new experimental plan of PEO coatings fabrication in an electrolyte with 500 g/L $Ca(NO_3)_2{\cdot}4H_2O$ with the use of a commercial DC power supply was designed and conducted. It was found that all formed coatings were porous and enriched in calcium and phosphorus, with a calcium-to-phosphorus ratio of about 0.2. The XPS results showed that the top 10-nm layer consists mainly of compounds containing titanium (Ti^{4+}), calcium (Ca^{2+}), as well as phosphorus and oxygen (PO_4^{3-} and/or HPO_4^{2-} and/or $H_2PO_4^{-}$,and/or $P_2O_7^{4-}$). To summarize, it should be noted that the obtained PEO porous coatings, which are enriched in calcium and phosphorus, may be used in the production of automotive and industrial catalysts and as biocompatible surfaces.

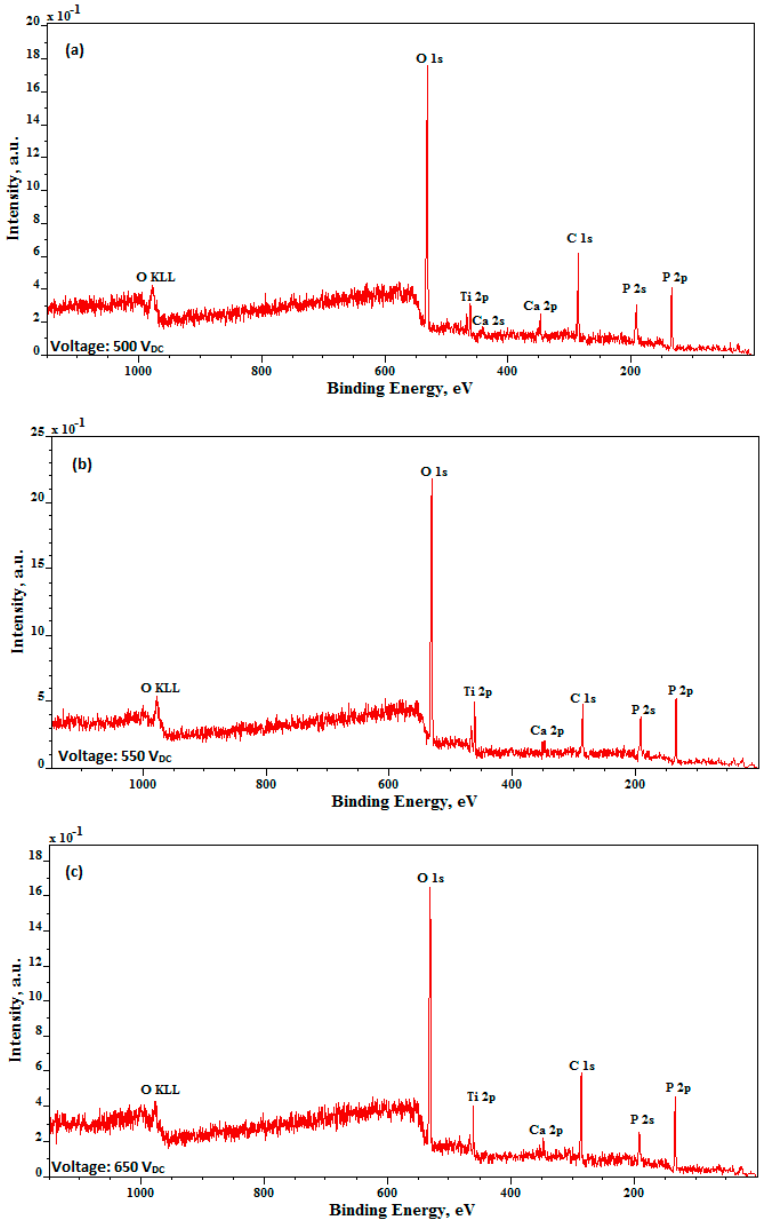

Figure 9. X-ray Photoelectron Spectroscopy (XPS) spectra of porous coatings formed on CP Titanium Grade 2 after PEO treatment at voltages of (**a**) 500 V_{DC}, (**b**) 550 V_{DC}, (**c**) 650 V_{DC}, in 500 g $Ca(NO_3)_2{\cdot}4H_2O$ in 1000 mL H_3PO_4 electrolyte.

4. Conclusions

Calcium- and phosphorus-enriched PEO coatings on CP Titanium Grade 2, obtained in electrolytes containing dissolved calcium nitrate tetrahydrate $Ca(NO_3)_2 \cdot 4H_2O$ in concentrated 85% analytically pure H_3PO_4 (98 g/mole) acid, may be characterized as follows:

(1) The coating obtained in the electrolyte with 10 g/L of calcium nitrate tetrahydrate in it at 450 ± 46 V with a pulsation of 300 Hz is not porous, whereas the coatings formed in the solutions with 300 and 600 g/L $Ca(NO_3)_2 \cdot 4H_2O$ are porous.

(2) The Ca/P ratio of the coatings, obtained by using a commercial DC power supply without pulsation, at 450 V, in an electrolyte containing 500 g/L of $Ca(NO_3)_2 \cdot 4H_2O$, is equal to 0.18 ± 0.01, which is slightly higher than that calculated for the coating formed at 450 ± 46 V with a pulsation of 300 Hz (0.15 ± 0.01).

(3) In the PEO coatings, three different sub-layers may be distinguished, i.e., the first with open pores, the second that is semi-porous and enriched in calcium, and the third, a transition sub-layer.

(4) The higher the amount of calcium nitrate tetrahydrate dissolved in an electrolyte, the thicker the second and third sub-layers become.

(5) The top surface of the PEO coatings consists of titanium (Ti^{4+}), calcium (Ca^{2+}), as well as phosphorus and oxygen (PO_4^{3-} and/or HPO_4^{2-} and/or $H_2PO_4^{-}$, and/or $P_2O_7^{4-}$).

Acknowledgments: This work was supported by a subsidy from Grant OPUS 11 of National Science Centre, Poland, with registration number 2016/21/B/ST8/01952, titled "Development of models of new porous coatings obtained on titanium by Plasma Electrolytic Oxidation in electrolytes containing phosphoric acid with addition of calcium, magnesium, copper and zinc nitrates".

Author Contributions: Krzysztof Rokosz and Tadeusz Hryniewicz conceived and designed the experiments; Krzysztof Rokosz, Sofia Gaiaschi, Patrick Chapon, Steinar Raaen, and Winfried Malorny performed the experiments; Krzysztof Rokosz, Tadeusz Hryniewicz, and Kornel Pietrzak analyzed the data; Krzysztof Rokosz, Tadeusz Hryniewicz, and Kornel Pietrzak contributed reagents, materials, analysis tools; Krzysztof Rokosz and Tadeusz Hryniewicz wrote the paper.

Conflicts of Interest: The authors declare no conflict of interest.

References

1. Aliasghari, S. Plasma Electrolytic Oxidation of Titanium. Ph.D. Thesis, The University of Manchester, Manchester, UK, 2014; p. 223.
2. Simka, W.; Sadowski, A.; Warczak, M.; Iwaniak, A.; Dercz, G.; Michalska, J.; Maciej, A. Modification of Titanium Oxide Layer by Calcium and Phosphorus. *Electrochim. Acta* **2011**, *56*, 8962–8968. [CrossRef]
3. Rokosz, K.; Hryniewicz, T.; Raaen, S.; Malorny, W. Fabrication and Characterisation of Porous Coatings Obtained by Plasma Electrolytic Oxidation. *J. Mech. Energy Eng.* **2017**, *1*, 23–30.
4. Puz', A.V.; Khlusov, I.A.; Opra, D.P. Functional Coatings Formed on the Titanium and Magnesium Alloys as Implant Materials by Plasma Electrolytic Oxidation Technology: Fundamental Principles and Synthesis Conditions. *Corros. Rev.* **2016**, *34*, 65–83.
5. Hryniewicz, T.; Rokosz, K.; Zschommler Sandim, H.R. SEM/EDX and XPS Studies of Niobium after Electropolishing. *Appl. Surf. Sci.* **2012**, *263*, 357–361. [CrossRef]
6. Rokicki, R.; Hryniewicz, T.; Konarski, P.; Rokosz, K. The Alternative, Novel Technology for Improvement of Surface Finish of SRF Niobium Cavities. *World Sci. News* **2017**, *74*, 152–163.
7. Rokosz, K.; Hryniewicz, T. Characteristics of Porous and Biocompatible Coatings Obtained on Niobium and Titanium-Niobium-Zirconium (TNZ) Alloy by Plasma Electrolytic Oxidation. *Mechanik* **2015**, *12*, 15–18. [CrossRef]
8. Rokosz, K.; Hryniewicz, T.; Matysek, D.; Dudek, Ł.; Valiček, J.; Harničarova, M.; Kušnerova, M.; Zschommler Sandim, H.R. SEM and EDS Analysis of Niobium Surface after Plasma Electrolytic Oxidation in Concentrated Phosphoric Acid within Copper Nitrate. In Proceedings of the 25th Anniversary International Conference on Metallurgy and Materials (METAL 2016), Brno, Czech Republic, 25–27 May 2016; pp. 1157–1162.

9. Rokosz, K.; Hryniewicz, T. Comparative SEM and EDX Analysis of Surface Coatings Created on Niobium and Titanium Alloys after Plasma Electrolytic Oxidation (PEO). *Teh. Vjesn. Tech. Gaz.* **2017**, *24*, 465–472.
10. Rokosz, K.; Hryniewicz, T.; Chapon, P.; Raaen, S.; Zschommler Sandim, H.R. XPS and GDOES Characterisation of Porous Coating Enriched with Copper and Calcium Obtained on Tantalum via Plasma Electrolytic Oxidation. *J. Spectr.* **2016**. [CrossRef]
11. Petković, M.; Stojadinović, S.; Vasilić, R.; Belča, I.; Kasalica, B.; Zeković, L. Plasma Electrolytic Oxidation of Tantalum. *Serb. J. Electr. Eng.* **2012**, *9*, 81–94. [CrossRef]
12. Sowa, M.; Kazek-Kęsik, A.; Socha, R.P.; Dercz, G.; Michalska, J.; Simka, W. Modification of Tantalum Surface via Plasma Electrolytic Oxidation in Silicate Solutions. *Electrochim. Acta* **2013**, *114*, 627–636. [CrossRef]
13. Petković, M.; Stojadinović, S.; Vasilić, R.; Zeković, Lj. Characterization of Oxide Coatings Formed on Tantalum by Plasma Electrolytic Oxidation in 12-tungstosilicic Acid. *Appl. Surf. Sci.* **2011**, *257*, 10590–10594. [CrossRef]
14. Stojadinović, S.; Jovović, J.; Petković, M.; Vasilić, R. Spectroscopic and Real-time Imaging Investigation of Tantalum Plasma Electrolytic Oxidation (PEO). *Surf. Coat. Technol.* **2011**, *205*, 5406–5413. [CrossRef]
15. Goularte, M.A.P.C.C.; Barbosa, G.F.; da Cruz, N.C.; Hirakata, L.M. Achieving Surface Chemical and Morphologic Alterations on Tantalum by Plasma Electrolytic Oxidation. *Int. J. Implant Dent.* **2016**, *2*, 1–12. [CrossRef] [PubMed]
16. Krząkala, A.; Młynski, J.; Dercz, G.; Michalska, J.; Maciej, A.; Nieużyla, L.; Simka, W. Modification of Ti-6Al-4V Alloy Surface by EPD-PEO Process in $ZrSiO_4$ Suspension. *Arch. Metall. Mater.* **2014**, *59*, 199–204. [CrossRef]
17. Rokicki, R.; Hryniewicz, T. Nitinol Surface Finishing by Magnetoelectropolishing. *Trans. Inst. Met. Finish.* **2008**, *86*, 280–285. [CrossRef]
18. Simka, W.; Nawrat, G.; Chlode, J.; Maciej, A.; Winiarski, A.; Szade, J.; Radwański, K.; Gazdowicz, J. Electropolishing and Anodic Passivation of Ti6Al7Nb Alloy. *Przem. Chem.* **2011**, *90*, 84–90.
19. Rokosz, K.; Hryniewicz, T.; Raaen, S.; Chapon, P. Investigation of Porous Coatings Obtained on Ti-Nb-Zr-Sn Alloy Biomaterial by Plasma Electrolytic Oxidation: Characterisation and Modelling. *Int. J. Adv. Manuf. Technol.* **2016**, *87*, 3497–3512. [CrossRef]
20. Rokosz, K.; Hryniewicz, T.; Raaen, S. SEM, EDS and XPS Analysis of Nanostructured Coating Obtained on NiTi Biomaterial Alloy by Plasma Electrolytic Oxidation (PEO). *Teh. Vjesn. Tech. Gaz.* **2017**, *24*, 193–198.
21. Rokosz, K.; Hryniewicz, T.; Raaen, S. Development of Plasma Electrolytic Oxidation for Improved Ti6Al4V Biomaterial Surface Properties. *Int. J. Adv. Manuf. Technol.* **2016**, *85*, 2425–2437. [CrossRef]
22. Rokosz, K.; Hryniewicz, T.; Raaen, S.; Chapon, P. Development of Copper-enriched Porous Coatings on Ternary Ti-Nb-Zr Alloy by Plasma Electrolytic Oxidation. *Int. J. Adv. Manuf. Technol.* **2017**, *89*, 2953–2965. [CrossRef]
23. Hryniewicz, T.; Rokosz, K.; Rokicki, R.; Prima, F. Nanoindentation and XPS Studies of Titanium TNZ Alloy after Electrochemical Polishing in a Magnetic Field. *Materials* **2015**, *8*, 205–215. [CrossRef] [PubMed]
24. Hryniewicz, T.; Rokosz, K.; Valiček, J.; Rokicki, R. Effect of Magnetoelectropolishing on Nanohardness and Young's Modulus of Titanium Biomaterial. *Mater. Lett.* **2012**, *83*, 69–72. [CrossRef]
25. Krupa, D.; Baszkiewicz, J.; Zdunek, J.; Sobczak, J.W.; Lisowski, W.; Smolik, J.; Słomka, Z. Effect of Plasma Electrolytic Oxidation in the Solutions Containing Ca, P, Si, Na on the Properties of Titanium. *J. Biomed. Mater. Res. B Appl. Biomater.* **2012**, *100*, 2156–2166. [CrossRef] [PubMed]
26. Yang, W.; Li, Q.; Liu, C.; Liang, J.; Peng, Z.; Liu, B. A Comparative Study of Characterisation of Plasma Electrolytic Oxidation Coatings on Carbon Steel Prepared from Aluminate and Silicate Electrolytes. *Surf. Eng.* **2017**, 1–9. [CrossRef]
27. Fei, C.; Hai, Z.; Chen, C.; Yangjian, X. Study on the Tribological Performance of Ceramic Coatings on Titanium Alloy Surfaces Obtained through Microarc Oxidation. *Prog. Org. Coat.* **2009**, *64*, 264–267. [CrossRef]
28. Hryniewicz, T.; Rokicki, R.; Rokosz, K. Co-Cr Alloy Corrosion Behaviour after Electropolishing and "Magnetoelectropolishing" Treatments. *Surf. Coat. Technol.* **2008**, *62*, 3073–3076. [CrossRef]
29. Hryniewicz, T.; Rokicki, R.; Rokosz, K. Corrosion and Surface Characterization of Titanium Biomaterial after Magnetoelectropolishing. *Surf. Coat. Technol.* **2008**, *203*, 1508–1515. [CrossRef]
30. Rokosz, K.; Hryniewicz, T. Effect of Magnetic Field on the Pitting Corrosion of Austenitic Steel Type AISI 304. *Ochr. Przed Koroz.* **2011**, *54*, 487–491.

31. Hryniewicz, T.; Rokosz, K. Corrosion Resistance of Magnetoelectropolished AISI 316L SS Biomaterial. *Anti-Corros. Methods Mater.* **2014**, *61*, 57–64. [CrossRef]
32. Echeverry-Rendón, M.; Galvis, O.; Giraldo, D.Q.; Pavón, J.; López-Lacomba, J.L.; Jiménez-Piqué, E.; Anglada, M.; Robledo, S.M.; Castaño, J.G.; Echeverría, F. Osseointegration Improvement by Plasma Electrolytic Oxidation of Modified Titanium Alloys Surfaces. *J. Mater. Sci. Mater. Med.* **2015**, *26*, 1–18. [CrossRef] [PubMed]
33. Rokicki, R.; Haider, W.; Hryniewicz, T. Influence of Sodium Hypochlorite Treatment of Electropolished and Magnetoelectropolished Nitinol Surfaces on Adhesion and Proliferation of MC3T3 Pre-osteoblast Cells. *J. Mater. Sci. Mater. Med.* **2012**, *23*, 2127–2139. [CrossRef] [PubMed]
34. Sowa, M.; Piotrowska, M.; Widziołek, M.; Dercz, G.; Tylko, G.; Gorewoda, T.; Osyczka, A.M.; Simka, W. Bioactivity of Coatings Formed on Ti-13Nb-13Zr Alloy Using Plasma Electrolytic Oxidation. *Mater. Sci. Eng. C Mater. Biol. Appl.* **2015**, *49*, 159–173. [CrossRef] [PubMed]
35. Hryniewicz, T. Concept of Microsmoothing in the Electropolishing Process. *Surf. Coat. Technol.* **1994**, *64*, 75–80. [CrossRef]
36. Hryniewicz, T.; Hryniewicz, Z. On the Solution of Equation of Diffusion in Electropolishing. *J. Electrochem. Soc.* **1989**, *136*, 3767–3769. [CrossRef]
37. Rokicki, R.; Hryniewicz, T. Enhanced Oxidation-Dissolution Theory of Electropolishing. *Trans. Inst. Met. Finish.* **2012**, *90*, 188–196. [CrossRef]
38. Hryniewicz, T.; Rokosz, K. Analysis of XPS Results of AISI 316L SS Electropolished and Magnetoelectropolished at Varying Conditions. *Surf. Coat. Technol.* **2010**, *204*, 2583–2592. [CrossRef]
39. Rokosz, K. *Electrochemical Polishing in the Magnetic Field*; Koszalin University of Technology Publishing House: Koszalin, Poland, 2012. (In Polish)
40. Rokosz, K.; Hryniewicz, T.; Raaen, S. XPS Analysis of Nanolayer Formed on AISI 304L after High-Voltage Electropolishing (HVEP). *Teh. Vjesn. Tech. Gaz.* **2017**, *24*, 321–326.
41. Rokicki, R.; Hryniewicz, T.; Rokosz, K. Modifying Metallic Implants by Magnetoelectropolishing. *Med. Device Diagn. Ind.* **2008**, *30*, 102–111.
42. Hryniewicz, T.; Rokicki, R.; Rokosz, K. Magnetoelectropolishing for Metal Surface Modification. *Trans. Inst. Met. Finish.* **2007**, *85*, 325–332. [CrossRef]
43. Hryniewicz, T.; Rokosz, K. Polarization Characteristics of Magnetoelectropolishing Stainless Steels. *Mater. Chem. Phys.* **2010**, *122*, 169–174. [CrossRef]
44. Rokosz, K.; Hryniewicz, T. XPS Measurements of LDX 2101 Duplex Steel Surface after Magnetoelectropolishing. *Int. J. Mater. Res.* **2013**, *104*, 1223–1232. [CrossRef]
45. Rokosz, K.; Hryniewicz, T.; Simon, F.; Rzadkiewicz, S. Comparative XPS Analysis of Passive Layers Composition Formed on AISI 304 L SS after Standard and High-Current Density Electropolishing. *Surf. Interface Anal.* **2015**, *47*, 87–92. [CrossRef]
46. Rokosz, K.; Lahtinen, J.; Hryniewicz, T.; Rzadkiewicz, S. XPS Depth Profiling Analysis of Passive Surface Layers Formed on Austenitic AISI 304L and AISI 316L SS after High-Current-Density Electropolishing. *Surf. Coat. Technol.* **2015**, *276*, 516–520. [CrossRef]
47. Rokosz, K.; Hryniewicz, T.; Simon, F.; Rzadkiewicz, S. Comparative XPS Analyses of Passive Layers Composition Formed on Duplex 2205 SS after Standard and High-Current-Density Electropolishing. *Teh. Vjesn. Tech. Gaz.* **2016**, *23*, 731–735.
48. Hryniewicz, T.; Rokosz, K. Investigation of Selected Surface Properties of AISI 316L SS after Magnetoelectropolishing. *Mater. Chem. Phys.* **2010**, *123*, 47–55. [CrossRef]
49. Rokosz, K.; Hryniewicz, T.; Raaen, S. Cr/Fe Ratio by XPS Spectra of Magnetoelectropolished AISI 316L SS Fitted by Gaussian-Lorentzian Shape Lines. *Teh. Vjesn. Tech. Gaz.* **2014**, *21*, 533–538.
50. Rokosz, K.; Hryniewicz, T.; Raaen, S. Characterization of Passive Film Formed on AISI 316L Stainless Steel after Magnetoelectropolishing in a Broad Range of Polarization Parameters. *Steel Res. Int.* **2012**, *83*, 910–918. [CrossRef]
51. Rokosz, K.; Hryniewicz, T. XPS Analysis of Nanolayers Obtained on AISI 316L SS after Magnetoelectropolishing. *World Sci. News* **2016**, *57*, 232–248.
52. Rokosz, K.; Hryniewicz, T.; Chapon, P.; Dudek, Ł. A New Approach to Porous PEO Coating Sub-layers Determination on the basis of GDOES Signals. *World Sci. News* **2016**, *57*, 289–299.

53. Hryniewicz, T.; Konarski, P.; Rokicki, R.; Valiček, J. SIMS Studies of Titanium Biomaterial Hydrogenation after Magnetoelectropolishing. *Surf. Coat. Technol.* **2012**, *206*, 4027–4031. [CrossRef]
54. Hryniewicz, T.; Konarski, P.; Rokicki, R.; Valiček, J. SIMS Analysis of Hydrogen Content in Near Surface Layers of AISI 316L SS after Electrolytic Polishing under Different Conditions. *Surf. Coat. Technol.* **2011**, *205*, 4228–4236. [CrossRef]
55. Rokosz, K.; Hryniewicz, T.; Pietrzak, K. Synthesis and characterisation of porous, calcium enriched coatings formed on Titanium via Plasma Electrolytic Oxidation. *World Sci. News* **2017**, *83*, 29–44.
56. Vallet-Regí, M.; Arcos Navarrete, D.A. *Nanoceramics in Clinical Use From Materials to Applications*, 2nd ed.; The Royal Society of Chemistry, Thomas Graham House, RSC Nanoscience & Nanotechnology No. 39: Cambridge, UK, 2016; p. 331. ISBN 978-1-78262-104-1.
57. Heimann, R.B.; Lehmann, H.D. *Bioceramic Coatings for Medical Implants Trends and Techniques*; Wiley-VCH Verlag GmbH & Co.: Weinheim, Germany, 2015; p. 467, ISBN 978-3-527-33743-9.
58. Hempel, F.; Finke, B.; Zietz, C.; Bader, R.; Weltmann, K.-D.; Polak, M. Antimicrobial Surface Modification of Titanium Substrates by Means of Plasma Immersion Ion Implantation and Deposition of Copper. *Surf. Coat. Technol.* **2014**, *256*, 52–58. [CrossRef]
59. Rokosz, K.; Hryniewicz, T.; Dudek, Ł.; Matysek, D.; Valiček, J.; Harničarova, M. SEM and EDS Analysis of Surface Layer Formed on Titanium After Plasma Electrolytic Oxidation in H_3PO_4 with the Addition of $Cu(NO_3)_2$. *J. Nanosci. Nanotechnol.* **2016**, *16*, 7814–7817. [CrossRef]
60. Rokosz, K.; Hryniewicz, T.; Dalibor, M.; Raaen, S.; Valiček, J.; Dudek, Ł.; Harničarova, M. SEM, EDS and XPS Analysis of the Coatings Obtained on Titanium after Plasma Electrolytic Oxidation in Electrolytes Containing Copper Nitrate. *Materials* **2016**, *9*, 318. [CrossRef] [PubMed]
61. Rokosz, K.; Hryniewicz, T.; Raaen, S.; Chapon, P.; Dudek, Ł. GDOES, XPS and SEM with EDS Analysis of Porous Coatings Obtained on Titanium after Plasma Electrolytic Oxidation. *Surf. Interface Anal.* **2016**, *49*, 303–315. [CrossRef]
62. Rokosz, K.; Hryniewicz, T.; Malorny, W. Characterisation of Porous Coatings Obtained on Materials by Plasma Electrolytc Oxidation. *Mater. Sci. Forum* **2016**, *862*, 86–95. [CrossRef]
63. Jelinek, M.; Kocourek, T.; Remsa, J.; Weiserová, M.; Jurek, K.; Mikšovský, J.; Strnad, J.; Galandáková, A.; Ulrichová, J. Antibacterial, Cytotoxicity and Physical Properties of Laser—Silver Doped Hydroxyapatite Layers. *Mater. Sci. Eng. C* **2013**, *33*, 1242–1246. [CrossRef] [PubMed]
64. Mishra, G.; Dash, B.; Pandey, S.; Mohanty, P.P. Antibacterial Actions of Silver Nanoparticles Incorporated Zn–Al Layered Double Hydroxide and its Spinel. *J. Environ. Chem. Eng.* **2013**, *1*, 1124–1130. [CrossRef]
65. Rajendran, A.; Pattanayak, D.K. Silver Incorporated Antibacterial, Cell Compatible and Bioactive Titania Layer on Ti Metal for Biomedical Applications. *RSC Adv.* **2014**, *106*, 61444–61455. [CrossRef]
66. Trujillo, N.A.; Oldinski, R.A.; Ma, H.; Bryers, J.D.; Williams, J.D.; Popat, K.C. Antibacterial Effects of Silver-Doped Hydroxyapatite Thin Films Sputter Deposited on Titanium. *Mater. Sci. Eng. C* **2012**, *32*, 2135–2144. [CrossRef]
67. Valiček, J.; Drzik, M.; Hryniewicz, T.; Harničarova, M.; Rokosz, K.; Kušnerova, M.; Barcova, K.; Brazina, D. Noncontact Method for Surface Roughness Measurement after Machining. *Meas. Sci. Rev.* **2012**, *12*, 184–188. [CrossRef]
68. Kušnerova, M.; Valiček, J.; Harničarova, M.; Hryniewicz, T.; Rokosz, K.; Palkova, Z.; Vaclavik, V.; Repka, M.; Bendova, M. A Proposal for Simplifying the Method of Evaluation of Uncertainties in Measurement Results. *Meas. Sci. Rev.* **2013**, *13*, 1–6. [CrossRef]
69. Teker, D.; Muhaffel, F.; Menekse, M.; Karaguler, N.G.; Baydogan, M.; Cimenoglu, H. Characteristics of Multi-Layer Coating Formed on Commercially Pure Titanium for Biomedical Applications. *Mater. Sci. Eng. C* **2015**, *48*, 579–585. [CrossRef] [PubMed]
70. Dzhurinskiy, D.; Gao, Y.; Yeung, W.-K.; Strumban, E.; Leshchinsky, V.; Chu, P.-J.; Matthews, A.; Yerokhin, A.; Maev, R.G. Characterization and Corrosion Evaluation of TiO_2:n-HA Coatings on Titanium Alloy Formed by Plasma Electrolytic Oxidation. *Surf. Coat. Technol.* **2015**, *269*, 258–265. [CrossRef]
71. Krupa, D.; Baszkiewicz, J.; Zdunek, J.; Smolik, J.; Słomka, J.; Sobczak, J.W. Characterization of the Surface Layers Formed on Titanium by Plasma Electrolytic Oxidation. *Surf. Coat. Technol.* **2010**, *205*, 1743–1749. [CrossRef]

72. Wang, H.-Y.; Zhu, R.-F.; Lu, Y.-P.; Xiao, G.-Y.; Zhao, X.-C.; He, K.; Yuan, Y.F.; Ying, L.; Ma, X.-N. Preparation and Properties of Plasma Electrolytic Oxidation Coating on Sandblasted Pure Titanium by a Combination Treatment. *Mater. Sci. Eng. C* **2014**, *42*, 657–664. [CrossRef] [PubMed]
73. Kazek-Kęsik, A.; Krok-Borkowicz, M.; Pamuła, E.; Simka, W. Electrochemical and Biological Characterization of Coatings Formed on Ti–15Mo Alloy by Plasma Electrolytic Oxidation. *Mater. Sci. Eng. C* **2014**, *43*, 172–181. [CrossRef] [PubMed]
74. Nelis, T.; Payling, R. *Practical Guide to Glow Discharge Optical Emission Spectroscopy*; Barnett, N.W., Ed.; RSC Analytical Spectroscopy Monographs; Royal Society of Chemistry: Cambridge, UK, 2002.
75. Pulsed RF Glow Discharge Optical Emission Spectrometry—Ultra Fast Elemental Depth Profiling, HORIBA Scientific, Printed in France—©HORIBA Jobin Yvon: 2014, p. 7. Available online: http://www.horiba.com/scientific/products/atomic-emission-spectroscopy/glow-discharge/ (accessed on 27 July 2017).
76. Gaiaschi, S.; Richard, S.; Chapon, P.; Acher, O. Real-time measurement in glow discharge optical emission spectrometry via differential interferometric profiling. *J. Anal. Atom. Spectrom.* **2017**, *32*, 1798–1804. [CrossRef]
77. Casa Software Ltd. CasaXPS: Processing Software for XPS, AES, SIMS and More. 2009. Available online: http://www.casaxps.com (accessed on 31 July 2007).
78. Wagner, C.D.; Naumkin, A.V.; Kraut-Vass, A.; Allison, J.W.; Powell, C.J.; Rumble, J.R., Jr. NIST Standard Reference Database 20, Version 3.4. 2003. Available online: http://srdata.nist.gov/xps (accessed on 31 July 2007).